

# Mechanical Properties of Thermoplastic Elastomeric Blends of Chitosan and Natural Rubber Latex

Vijayalakshmi Rao, Jobish Johns

Department of Materials Science, Mangalore University, Mangalagangothri 574199, India

Received 4 April 2007; accepted 30 August 2007

DOI 10.1002/app.27265

Published online 5 November 2007 in Wiley InterScience (www.interscience.wiley.com).

**ABSTRACT:** Thermoplastic chitosan/natural rubber blends (Cs/NR) were prepared from natural rubber latex and chitosan by solution casting technique. The blends were characterized by mechanical analysis (stress–strain) and the mechanical properties were found to vary with chitosan/natural rubber ratios. Experimental values were compared with different theoretical models. Effect of thermal aging on mechanical

properties was also investigated. Dicumyl peroxide was used as the crosslinking agent. The effect of crosslinking on mechanical properties of Cs/NR has also been studied. © 2007 Wiley Periodicals, Inc. *J Appl Polym Sci* 107: 2217–2223, 2008

**Key words:** natural rubber latex; chitosan; mechanical properties; thermoplastic elastomeric blend

## INTRODUCTION

Blending of two polymers usually gives rise to a new material having better balance of properties than obtainable with a single polymer.<sup>1</sup> The emergence of thermoplastic elastomers is one of the important developments in the field of polymer science and technology in recent years. Thermoplastic elastomers are a new class of materials which combine the properties of rubber with the ease of processability of thermoplastics. One type of fast-growing thermoplastic elastomer which is easier to process is made by blending rubber and plastic in definite proportions. Characteristically, this is a family of materials consisting of a rubber soft segment which gives rise to elastomeric properties and a crystalline hard segment which acts as crosslink and fillers.

Chitosan (Fig. 1) is a partially acetylated glucosamine obtained by deacetylation of chitin, one of the most abundant natural polymers.<sup>2–4</sup> As a polysaccharide of natural origin, chitosan has many useful features such as nontoxicity, biocompatibility, biodegradability, good mechanical strength, and antimicrobial properties.<sup>5,6</sup> Chitosan can be used in different areas from health care to agriculture and dyes for fabrics, and it is soluble in most diluted acids.<sup>7</sup> Chitosan has a high modulus of elasticity, owing to the higher glass transition temperature and crystallinity.<sup>8,9</sup> Natural rubber (NR), *cis*-1,4-polyisoprene (Fig. 2), occurs in several plant species, but its most important source is the “*Hevea brasiliensis*” tree, which

accounts for over 99% of the world’s natural rubber production. Natural rubber is extracted as a latex or ‘milk’, viz. an aqueous emulsion or dispersion of the natural polymer (~96 wt % of solids) and other substances, such as proteins (~1%), lipids (~3%), and traces of potassium, magnesium, and copper. An adsorbed layer of protein and phospholipids stabilizes the rubber particles.<sup>10</sup> Natural rubber is characterized by good elastic properties, good resilience, and damping behavior but poor chemical resistance and processability. The unique mechanical properties of NR results from both its highly stereoregular microstructure and the rotational freedom of the  $\alpha$ -methylene C–C bonds and from the entanglements resulting from the high molecular weight which contributes to its high elasticity.<sup>11</sup> Chitosan has been blended with polymers like polymethyl methacrylate, PVA, cellulose, PVP, starch, etc.<sup>4,7,12</sup> Several researchers have reported the studies on blends of natural rubber with other polymers.<sup>10,13–15</sup> The mechanical properties of these blends depend on properties of individual components, interaction between them, and morphology of blends. In this article, we report the mechanical properties of blends of thermoplastic chitosan with latex of *Hevea brasiliensis*. To our knowledge, till date, no studies have been conducted on the chitosan/natural rubber blends (Cs/NR).

## EXPERIMENTAL

### Materials

Purified chitin was purchased from HiMedia Laboratories Pvt., Mumbai, India and its average molecular weight was 400,000 g/mol. The natural rubber latex was used directly as extracted from the tree (*Hevea*

Correspondence to: V. Rao (vijrao@yahoo.com).

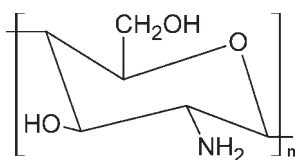


Figure 1 Structure of chitosan.

*brasiliensis*), cultivated around the belt of Western Ghats, Karnataka, India. The latex was stabilized by adding 2.5% of a 28%, approximately 10% ammonium hydroxide solution. The dry rubber content was determined by drying the emulsion in an oven at 110°C for 12 h and is found to be 40%. Dicumyl peroxide (DCP) was also purchased from HiMedia Laboratories Pvt. Mumbai, India.

### Preparation of chitosan and chitosan solution

Chitin was dispersed in 50% (w/w) NaOH solution and heated at 100°C for 2 h. Then the mixture was cooled to room temperature, filtered, and washed with water several times until the filtrate was neutral. The chitosan sample obtained was dried in oven at 60°C for 48 h. The chitosan solution was prepared by dissolving chitosan in 2% (v/v) acetic acid.

### Preparation of Cs/NR

The blends were prepared by mixing Chitosan and natural rubber latex to get a homogeneous solution. The mixture was cast on a Petri dish at 45°C for 48 h. The films were prepared by compressing these casted samples at 140°C and a pressure of 10 ton for 10 min in a hydraulic press. The film thickness was 2–2.5 mm. Chitosan crosslinked rubber blend was prepared by adding 3% DCP to the blend solution, followed by drying and compression.

### Mechanical tests

The tensile testing of the samples was performed according to ASTM D 412 method using dumb-bell

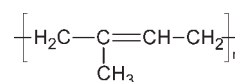


Figure 2 Structure of Natural Rubber.

shaped test specimens at a crosshead speed of 500 mm/min using a Universal testing machine (UTM, SHIMADZU AGI). The experiments were conducted at room temperature. Stress–strain curves were plotted for each blend. These tests provided the ultimate tensile strength (UTS), strain at break, and elastic modulus. Hardness (Shore A) was measured according to ASTM D 2240 method using a hardness tester (Shore A durometer). All the values reported are obtained from at least four test results.

### Aging studies

The aging of samples was carried out by keeping the samples in a hot air oven for 10 days at 55°C. After that, the mechanical properties of the samples were studied using UTM.

## RESULTS AND DISCUSSION

The results related to UTS, elongation at break ( $\epsilon_{\text{break}}$ ), and modulus at different elongations (50%, 100%) are presented in Table I. The stress–strain curves of Cs/NR are given in Figure 3. These curves illustrate the deformation pattern of different blends. The studies have been limited to 50/50 Cs/NR, as above this volume fraction, the films were found to be brittle and were difficult to carry out mechanical testing. The stress–strain curve shows a gradual transition from rubbery to plastic nature as chitosan content increases. This can be understood from the decrease in elongation. As the percentage of chitosan increases, the chain flexibility of the system is highly restricted and the elongation is drastically reduced.

The addition of chitosan to the rubber decreases softening as shown by the corresponding increase in modulus (Fig. 4). The UTS increases with the addition of chitosan (Cs) up to 0.35 volume fraction

TABLE I  
Mechanical Properties of Chitosan (Cs) and Natural rubber (NR) Blends

Sample	Ultimate tensile strength (MPa)	Elongation at break (%)	Young's modulus at 50% elongation (MPa)	Young's modulus at 100% elongation (MPa)
0 100 Cs NR	0.46	597.46	0.20	0.29
10 90 Cs NR	0.98	456.66	0.43	0.57
15 85 Cs NR	1.93	438.61	0.58	0.78
20 80 Cs NR	1.78	278.71	0.95	0.72
35 65 Cs NR	3.25	245.38	1.98	2.46
50 50 Cs NR	0.96	453.99	0.46	0.035
10 90 Cs NR (vulcanized)	3.40	23.5	0.035	1.17

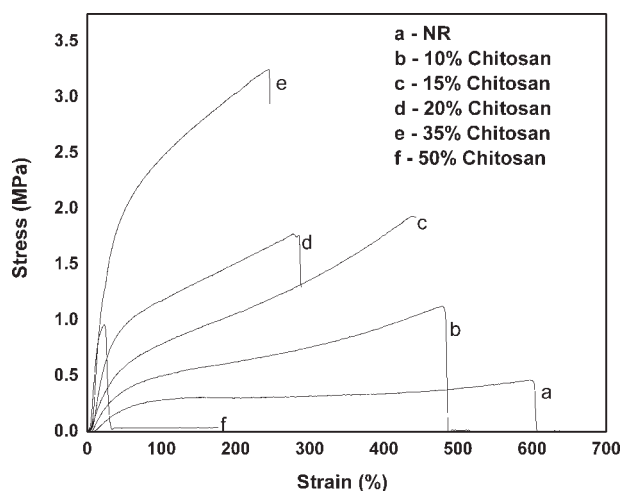


**Figure 3** Stress–strain curves showing effect of blend ratio.

and then decreases (Fig. 5). The UTS of Cs10 blend increases to 246% by vulcanizing with 3% DCP and its modulus increases to 149%, whereas the elongation at break decreases with increasing the percentage of chitosan (Fig. 5). The hardness (Shore A) of the blend increases by the addition of chitosan to natural rubber (Fig. 6, Table II). As hardness increases, the elongation at break decreases.

Mechanical properties of thermally aged six samples of Cs/NR have been studied and the data is presented in Table III. It is important to maintain the physical properties of latex goods during service. Figure 7 shows the stress–strain curves of unaged and aged blend samples for different blend ratios. Figures 8 and 9 exhibit that for blend samples aged at 55°C the tensile properties have improved. This is due to thermal crosslinking within the elastomeric phase.<sup>16–18</sup> Thermal crosslinking has been confirmed from the

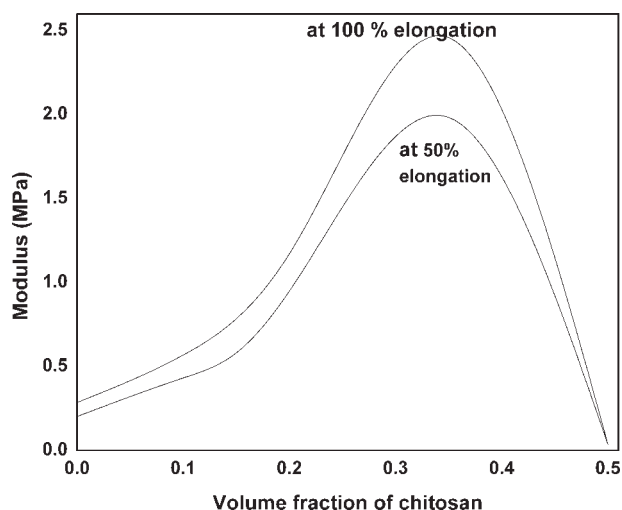


**Figure 4** Effect of blend ratio on modulus at 100 and 50% elongation.

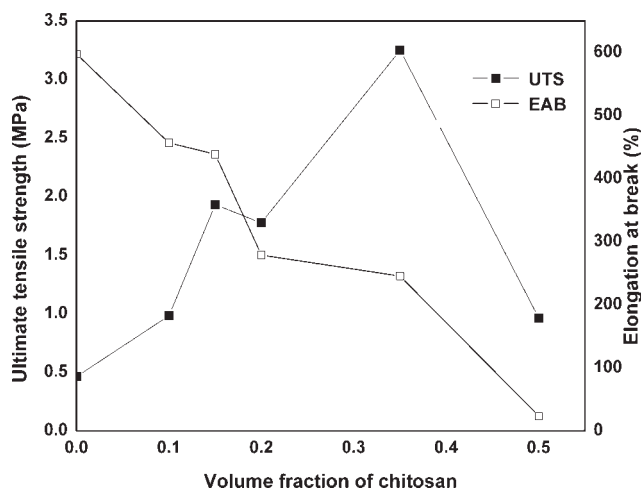


**Figure 5** Effect of blend ratio on ultimate tensile strength (UTS) and elongation at break.

swelling studies. The swelling rate decreased by 66% for the aged sample compared to the unaged sample. This is an evidence for the thermal crosslinking during aging.

The mechanical properties of two-phase composites made up of a continuous polymer phase and particulate filler phase have been studied in great detail. As a result, a variety of models are available to describe the modulus, tensile strength, and elongation at break as a function of filler volume fraction.

Different models like parallel, series, and Halpin-Tsai models have been used to predict the mechanical properties of these blends.<sup>13</sup> The highest-upper bound parallel model is given by the rule of mixtures,

$$M = M_1\phi_1 + M_2\phi_2 \quad (1)$$

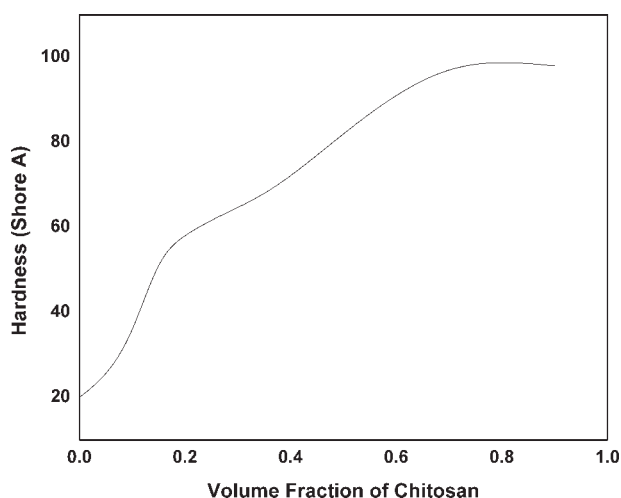


**Figure 6** Effect of blend ratio on hardness.

**TABLE II**  
Hardness of Chitosan (Cs) and Natural Rubber (NR) Blends

Sample	Hardness (Shore A)
0 100 Cs NR	20
10 90 Cs NR	36
15 85 Cs NR	51
20 80 Cs NR	58
35 65 Cs NR	68
50 50 Cs NR	82
70 30 Cs NR	97
10 90 Cs NR	98
90 10 Cs NR (vulcanized)	39

where  $M$  is any mechanical property of the blend.  $M_1$  and  $M_2$  are the mechanical properties of the components 1 and 2 respectively, and  $\phi_1$  and  $\phi_2$  are their corresponding volume fractions. In this model, the components are arranged parallel to one another, so that the applied stress elongates each component by the same extent. In the lowest-bound series model, the blend components are arranged in series and the equation is given as follows,

$$\frac{1}{M} = \frac{\phi_1}{M_1} + \frac{\phi_2}{M_2} \quad (2)$$

Parameters  $M$ ,  $M_1$ ,  $M_2$ ,  $\phi_1$  and  $\phi_2$  are the same as in the upper limit model.

According to Halpin-Tsai equation,

$$\frac{M_1}{M} = \frac{[1 + A_i B_i \phi_2]}{[1 - B_i \phi_2]} \quad (3)$$

where

$$B_i = \frac{\left(\frac{M_1}{M_2}\right) - 1}{\left(\frac{M_1}{M_2}\right) + A_i} \quad (4)$$

In these models subscripts 1 and 2 correspond to the continuous and dispersed phases, respectively. The constant  $A_i = 0.66$  when elastomers forms the dispersed phase in continuous hard matrix. On the other hand, if the hard material forms the dispersed

phase in a continuous elastomer matrix, then  $A_i = 1.5$ . In the case of incompatible blends, generally the experimental value is between the parallel upper bound ( $M_U$ ) and the series lower bound ( $M_L$ ) values.

Figure 10 shows the experimental and theoretical curves of modulus of the blend. It can be seen that the experimental data is overlapping with lower bound series and Halpin-Tsai models.

Sato and Furukawa have developed an expression for the modulus for the case where the adhesion is so poor that the polymer matrix pulls away from the filler surface to give cavities around the filler particles. Their equation is

$$E = E_m \left[ \left( 1 + \frac{\phi^{2/3}}{2 - 2\phi^{1/3}} \right) (1 - \psi\zeta) - \frac{\phi^{2/3}\psi\zeta}{(1 - \phi^{1/3})\phi} \right] \quad (5)$$

where

$$\psi = \left( \frac{\phi}{3} \right) \frac{1 + \phi^{1/3} - \phi^{2/3}}{1 - \phi^{1/3} + \phi^{2/3}} \quad (6)$$

and  $\zeta$  is the adhesion parameter;  $\zeta = 1$  for poor adhesion and  $\zeta = 0$  for perfect adhesion.

Figure 11 shows that the experimental curve is close to the curve plotted for  $\zeta = 0$  from the eq. (5) and the curve plotted for  $\zeta = 1$  is far away from the experimental curve. This shows that there is a considerable adhesion between the two phases in the blend.

To understand the level of interaction between the components in Cs/NR, models were tried to predict the tensile strength values.<sup>19-21</sup> These models include:

1. Nielsen's first power law model:

$$\frac{\sigma_b}{\sigma_p} = (1 - \phi_1)s \quad (7)$$

2. Nielsen's two-third power law model:

$$\frac{\sigma_b}{\sigma_p} = (1 - \phi_1^{2/3})s' \quad (8)$$

**TABLE III**  
Mechanical Properties of Aged Chitosan (Cs) and Natural rubber (NR) Blends

Sample	Ultimate tensile strength (MPa)	Elongation at break (%)	Young's modulus at 50% elongation (MPa)	Young's modulus at 100% elongation (MPa)
0 100 CsNR	1.61	1113.08	0.20	0.32
10 90 CsNR	1.82	479.75	0.53	0.72
15 85 CsNR	2.18	415.17	0.62	0.84
20 80 CsNR	2.17	331.31	0.94	1.19
35 65 CsNR	3.37	122.21	2.77	3.30
50 50 CsNR	2.33	48.5	2.24	-

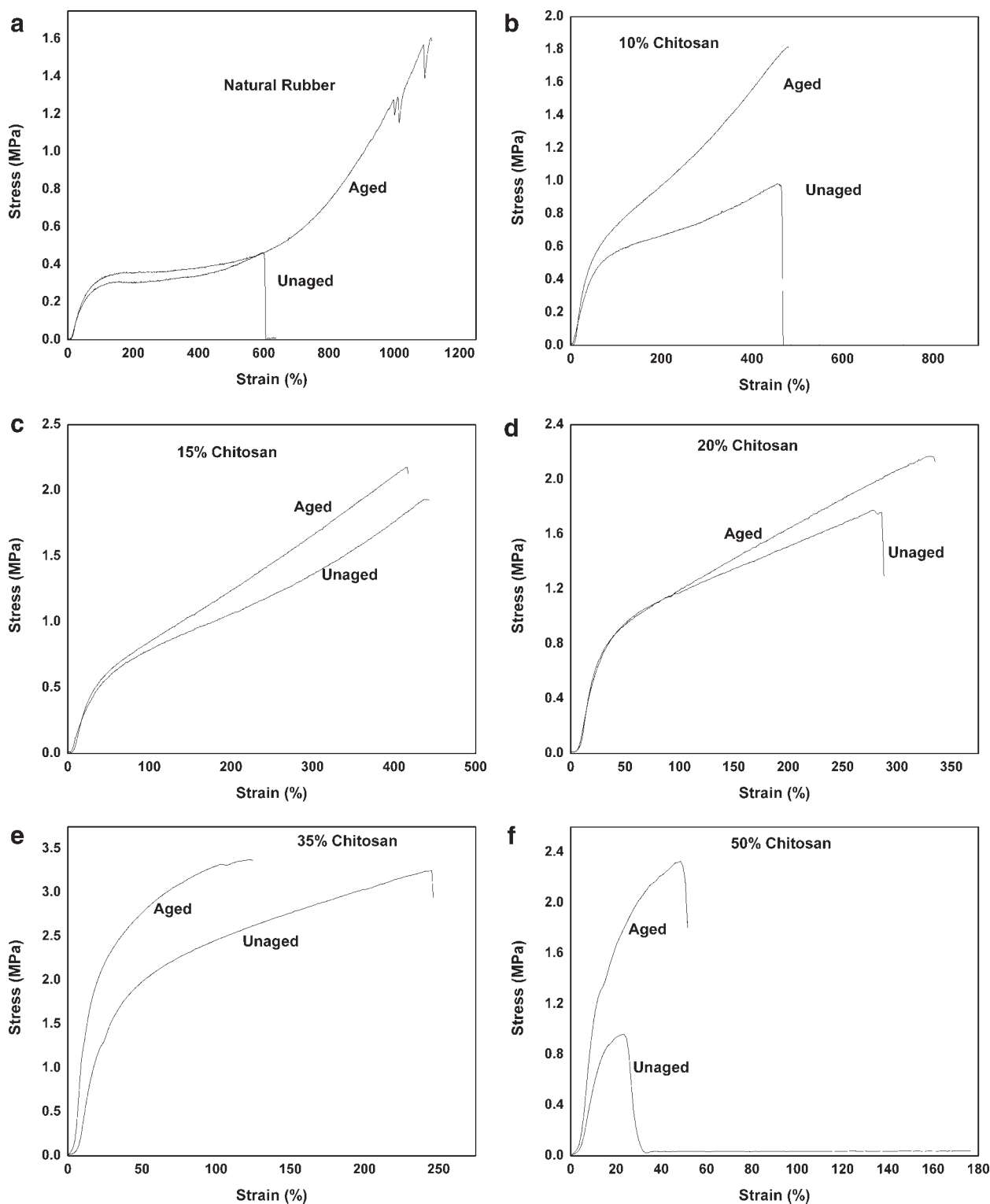


**Figure 7** Stress–strain curves of different blend ratios for aged and unaged samples. (a) Pure natural rubber, (b) Cs10/NR90, (c) Cs15/NR85, (d) Cs20/NR80, (e) Cs35/NR65, (f) Cs50/NR50.

3. Nicolais-Narkí's model:

$$\frac{\sigma_b}{\sigma_p} = (1 - K_b \phi_1^{2/3}) \quad (9)$$

where  $\sigma_b$  and  $\sigma_p$  represent the tensile strength of the blend and the major component of the blend,

respectively,  $\phi_1$  is the volume fraction of the major phase.  $s$  and  $s'$  are Nielsen's parameters in the first and two-third power law models, respectively, and  $K_b$  is an adhesion parameter.  $s$  and  $s'$  account for the weakness in the structure brought about by the discontinuity in stress

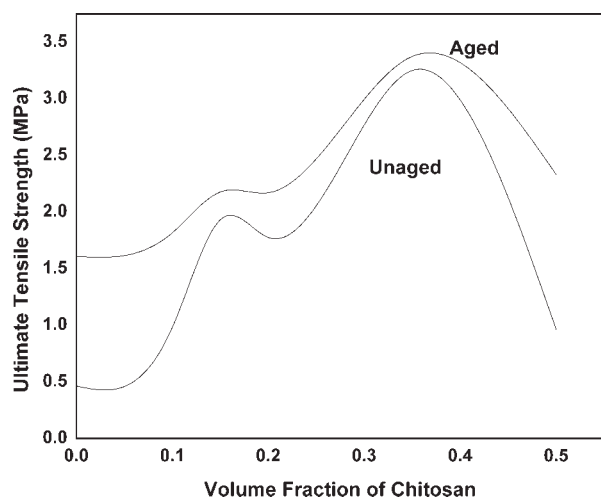


Figure 8 Effect of aging on ultimate tensile strength.

transfer and generation of stress concentration at the interface in the case of blends. The values of  $s$  and  $s'$  are unity in the case of no stress concentration effect. The value of  $K_b$  is 1.21 for spherical inclusions of the minor phase having no adhesion. Plots of relative tensile strength versus volume fraction of the blends predicted using the three models are presented in Figure 12. The experimental values of  $\sigma_b/\sigma_p$  predicted from eqs. (7)–(9) and the values of  $s$ ,  $s'$  and  $K_b$  have been calculated from the experimental  $\sigma_b/\sigma_p$  values are shown in Table IV.

From Figure 12, the interesting fact is that, the experimental values lie above the theoretical curve and the parameter  $K_b$ , in the Nicolais-Narkis model which accounts for the adhesion between the filler particles and the matrix shows negative values, which indicates that there is significant adhesion between the phases in the blend.

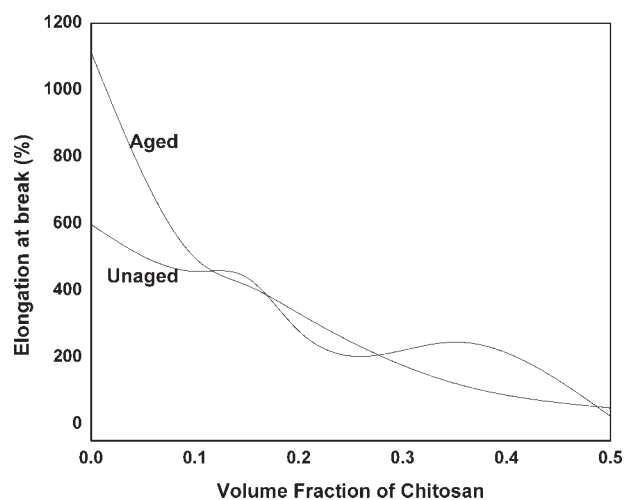


Figure 9 Effect of aging on elongation at break.

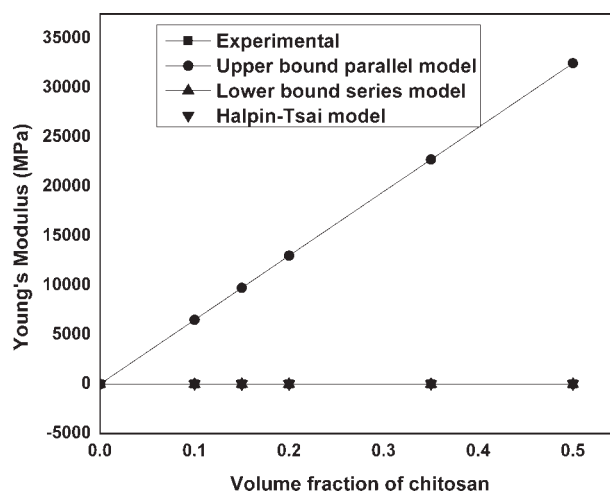


Figure 10 Theoretical modeling of Young's modulus related to compatibility.

The decrease in elongation at break in filled-polymer composites is due to the fact that the deformation of the filler is generally much less than that of the polymer matrix; thus, the filler forces the matrix to deform more than the overall deformation of the composite. A basic model that describes the elongation at break was developed by Nielsen.<sup>19,20</sup> For the case of perfect adhesion, under the assumption that the polymer breaks at the same elongation in the filled system as in the neat polymer, the elongation at break is given by

$$\varepsilon = \varepsilon_m(1 - \phi^{1/3}) \quad (10)$$

In the case of poor adhesion, the elongation is expected to decrease more gradually than in the case of perfect adhesion.

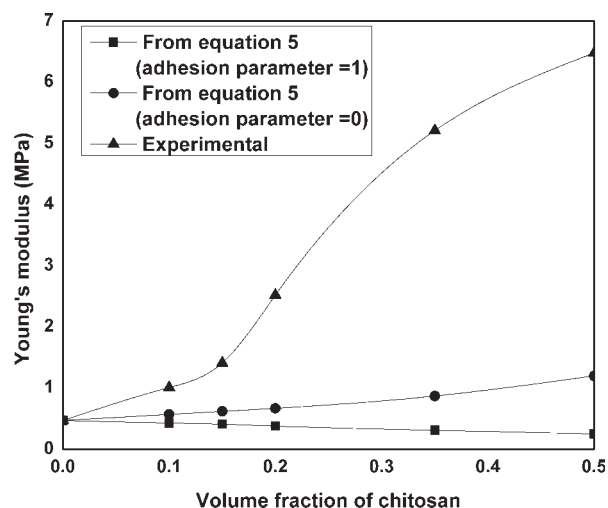


Figure 11 Theoretical modeling of Young's modulus related to adhesion.

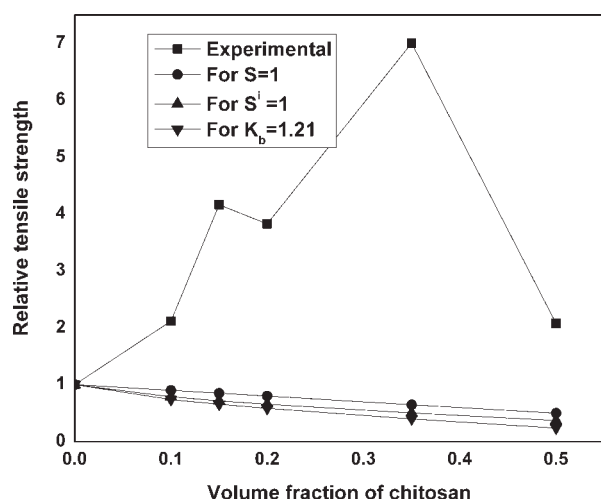


Figure 12 Theoretical modeling of relative tensile strength.

Another simple theoretical analysis for the elongation at break of elastomer composites is given by Smith as follows:

$$\varepsilon = \varepsilon_m(1 - 1.105\phi^{1/3}) \quad (11)$$

where  $\varepsilon$  and  $\varepsilon_m$  are the elongations at break of the composite and the unfilled polymer, respectively, and  $\phi$  is the volume fraction of chitosan.

The experimental and theoretical values of elongation at break are plotted in Figure 13. The result suggests that there is significant adhesion between the matrix and chitosan particles.

## CONCLUSIONS

Chitosan has been successfully blended with natural rubber latex by solution casting method. The blended samples show enhanced mechanical properties. Aging of Cs/NR at 55°C for 10 days increased the tensile strength due to thermal crosslinking in the natural rubber phase. The 35/65 chitosan/NR blend possesses maximum tensile strength among the blend ratios studied. From the study of mechanical properties, it is found that there is good adhesion

TABLE IV  
Relative Tensile Strength and Adhesion Parameters  
of NR Rich Blends

Blend	$\sigma_b/\sigma_p$	$s$	$s'$	$K_b$
0 100 Cs NR	1	1	1	—
10 90 Cs NR	2.12	2.35	2.70	-5.19
15 85 Cs NR	4.16	4.90	5.80	-11.20
20 80 Cs NR	3.83	4.78	5.81	-8.26
35 65 Cs NR	7.00	10.77	13.91	-12.09
50 50 Cs NR	2.07	4.15	5.60	-1.70

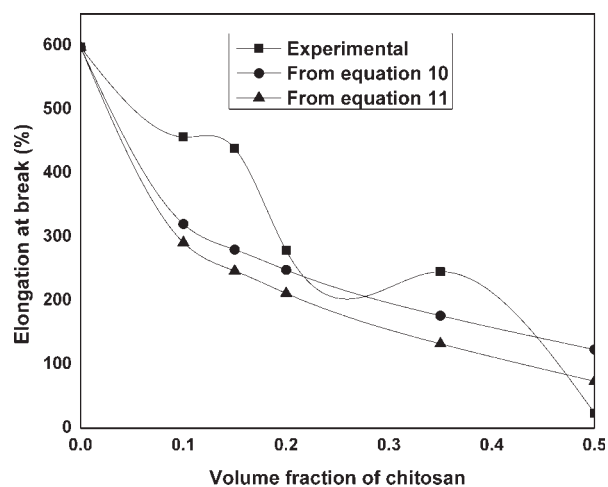


Figure 13 Theoretical modeling of elongation at break.

between the two phases. Blend with DCP shows increase in mechanical properties.

## References

1. Utracki, L. A. *Polymer Alloys and Blends*; Asian Books Private Ltd.: India, 1989; p 13.
2. Casimiro, M. H.; Leal, J. P.; Gil, M. H. *Nucl Instrum Methods Phys Res Sect B* 2005, 236, 482.
3. Wanjun, T.; Cunxin, W.; Donghua, C. *Polym Degrad Stab* 2005, 87, 389.
4. Cardenas, G.; Miranda, S. P. *J Chil Chem Soc* 2004, 49, 291.
5. Tolaimate, A.; Desbrieres, J.; Rhazi, M.; Alagui, A. *Polymer* 2003, 44, 7939.
6. Oliveira, B. F.; Santana, M. H. A.; Re, M. I. *Braz J Chem Eng* 2005, 22, 353.
7. Yilmaz, E.; Ozalp, D.; Yilmaz, O. *Int J Polym Anal Char* 2005, 10, 329.
8. Chen, C.; Dong, L.; Cheung, M. K. *Eur Polym J* 2005, 41, 958.
9. Yusong, W. U.; Seo, T.; Maeda, S.; Dong, Y.; Sasaki, T.; Irie, S. *J Polym Sci Part B: Polym Phys* 2004, 42, 2747.
10. Carvalho, A. J. F.; Job, A. E.; Alves, N.; Curvelo, A. A. S.; Gandini, A. *Carbohydr Polym* 2003, 53, 95.
11. Kalaprasad Gopalan Nair, Alain Dufresne. *Biomacromolecules* 2003, 4, 657.
12. Radhakumary, C.; Nair, P. D.; Mathew, S.; Reghunandhan Nair, C. P. *Trends Biomater Artif Organs* 2005, 18, 117.
13. Ashaletha, R.; Kumaran, M. G.; Thomas, S. *Eur Polym J* 1999, 35, 253.
14. Roy Choudhury, N.; Chaki, T. K.; Dutta, A.; Bhowmick, A. K. *Polymer* 1989, 30, 2047.
15. Neoh, S. B.; Hashim, A. S. *J Appl Polym Sci* 2004, 93, 1660.
16. Mathew, A. P.; Packirisamy, S.; Thomas, S. *Polym Degrad Stab* 2001, 72, 423.
17. Radhesh Kumar, C.; Fuhrmann, I.; Karger-Kocsis, J. *Polym Degrad Stab* 2002, 76, 137.
18. Geethamma, V. G.; Pothan, L. A.; Rhao, B.; Neelakantan, N. R.; Thomas, S. *J Appl Polym Sci* 2004, 94, 96.
19. Nielsen, L. E. *J Appl Polym Sci* 1966, 10, 97.
20. Bliznakov, E. D.; White, C. C.; Shaw, M. T. *J Appl Polym Sci* 2000, 77, 3220.
21. Nicolais, L.; Narkis, M. *Polym Eng Sci* 1971, 11, 194.